ACS OMEGA

Open Access

http://pubs.acs.org/journal/acsodf

Article

MnO_2/Ni−Cu-Plated Polyester Fabric as a Free-Standing Electrode in Supercapacitor Applications

Sheila Shahidi, Fatma Kalaoglu, Leila Naji, Alireza Rahmanian, and Rattanaphol Mongkholrattanasit*

Cite This: *ACS Omega* 2025, 10, 7091−7101

Read Online

ACCESS | Metrics & More | Article Recommendations

ABSTRACT: The main objective of this research is to investigate the electrochemical characteristics of Ni−Cu-plated polyester when MnO_2 is deposited on it and serves as a flexible electrode. For this purpose, the Ni−Cu-plated polyester electrode fabrics prepared in this way were deposited with MnO_2 over different immersion times. The conductive polyester electrode that was prepared underwent immersion in an aqueous solution of $KMnO_4$ (0.1 M) for durations of 5, 10, and 30 min. The electrical resistance of the prepared samples was measured using a two-point probe technique. Additionally, the electrochemical properties of the Ni−Cu-plated polyester with MnO_2 deposition were examined using a three-electrode cell setup under ambient conditions. The surface structure and elemental composition of the sample electrodes were examined with a scanning electron microscope (SEM). In this research, the asymmetric supercapacitor cell (ASC) consisting of a Ni−Cu/MnO_2-deposited textile as the cathode electrode and active carbon-coated activated carbon cloth as the anode electrode was assembled. Also, the symmetric supercapacitor cell (SSC) using Ni−Cu/MnO_2 deposited polyester as both the anode and cathode was assembled. Cyclic voltammetry (CV), galvanostatic charging−discharging (GCD), and electrochemical impedance spectroscopy (EIS) measurements were utilized to assess and compare the electrochemical performance. The areal specific capacitances of the ASC at current densities of 2, 4, 8, and 16 mA cm^{-2} were calculated to be 558.6, 481.9, 435.5, and 330 mF cm^{-2}, respectively. In comparison, the achieved storage results related to ASC are far higher than those of SSC. The results are discussed in the text in detail.

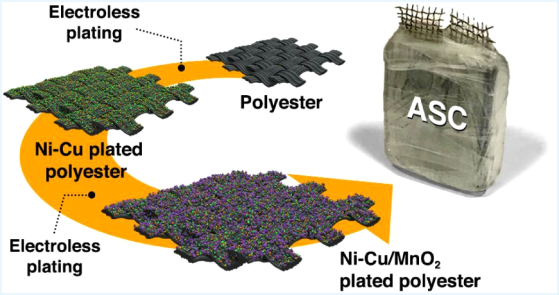

1. INTRODUCTION

Supercapacitors hold a significant place among advanced energy storage systems because of their unique capability to bridge the power−energy gap between conventional dielectric capacitors and battery fuel cells.[1] Supercapacitors are characterized by special properties such as high power density, high charge−discharge rate with an unstable energy source, reliable cycle life, cost-effectiveness, and well-being. They have demonstrated impressive capabilities in backup systems for computer storage, portable consumer electronics, electric or hybrid modes of transportation, and the management of power and energy in engineering applications.[2]

Currently, supercapacitors are very popular in portable electronics. Wearable electronics represent a developed class of materials that retain exclusive properties, for example, great flexibility, foldability, rotation, and lightweight. Because of these features, they find promising uses in sports cloths, army uniforms, portable power, and biomedical materials such as gowns, bandages, and monitoring tools. The presence of flexible and wearable electronic gadgets has impacted our everyday routines.[1,2] With the rapid advancement of wearable electronic devices like personal health monitors, flexible screens, and wearable sensors, there is a growing demand for energy storage materials and devices.[2,4]

Intelligent textiles and goods derived from them have become increasingly widespread in recent years.[1] In order to cover electricity needs, flexible energy storage in a variety of forms is being researched.[5] Textile-based supercapacitors make up an important subset of flexible supercapacitors. They have received extensive scrutiny because of their potential to advance eco-friendly, flexible, and wearable electronics.[1] The use of textile materials proves promising for meeting the requirements for the development of flexible energy storage, mainly due to their exceptional mechanical resilience, low weight, large surface area, and promising commercial viability.[6] For flexible energy devices, the key is to obtain suitable flexible electrodes, which have been extensively studied in recent years.[7] Besides carbon-based electrode materials, pseudocapacitive materials such as transition metal oxides and conductive organic polymers demonstrate considerably higher specific

Received: November 8, 2024
Revised: January 27, 2025
Accepted: February 3, 2025
Published: February 10, 2025

capacitance due to the quick and reversible redox reactions occurring on the surface of electroactive species.[8]

Among the many pseudocapacitive materials, metal oxides, such as MnO_2, NiO, and Co_3O_4, are well-suited for creating high-performance supercapacitors due to their high theoretical capacity. When compared, pseudocapacitive materials like transition metal oxides and conductive polymers demonstrate greater capacitance than carbon-based materials. Pseudocapacitive materials can store charges via highly reversible redox reactions.[9] However, their low conductivity, significant volume changes, and complex manufacturing processes make them seldom used for producing high-performance textile-based electrodes. Therefore, it is a major task to produce and prepare conductive textiles.[10]

Manganese dioxide (MnO_2), a transition metal oxide, has demonstrated excellent characteristics for achieving high-performance supercapacitors (SCs) due to its high theoretical capacitance (1400 F g^{-1}) and eco-friendly nature. It is commonly utilized in the fabrication of high-performance supercapacitors, enabling rapid charge and discharge rates.[11] Nanostructured MnO_2 provides numerous active sites and suitable channels for ion intercalation, while carbon cloth (CC) serves as elastic buffering layers to alleviate the strain within MnO_2 during repeated charge−discharge cycles.[12,13] Nevertheless, the inherently low conductivity of textiles requires adding a conductive coating to apply pseudocapacitive materials onto textile surfaces, limiting their effectiveness for high-energy devices.[6] Conductive substrates (current collectors) are typically necessary to provide support for the nanostructured active materials and enhance the charge transfer. Wearable electronics often opt for flexible supercapacitors equipped with current collectors like carbon cloths, metal foils, metal foams, and metal fabrics.[14]

For designing flexible supercapacitors, bottom-up and top-down methods have been recognized in recent research works. In the bottom-up approach, natural or synthetic fibers are converted into electrode fibers using different processes, for example, carbonization, which can then be interwoven into energy storage devices in a further step. In contrast, the top-down methodology transforms already manufactured materials into energy storage. Due to the electrically insulating properties of fabrics, this approach generally uses a two-step process. Initially, fabrics undergo a coating process with a conductive material. Subsequently, various active materials are deposited using different methods onto the surface of these already conductive fabrics in a second step, aiming to enhance capacitive performance.[15] In previous research, a Ni−Cu-plated polyester fabric with nanoscale structures was synthesized and used as a flexible electrode. The GCD test indicated that the Ni−Cu-plated polyester fabric had a specific capacity of 450 mF cm^{-2} at a current density of 7.5 mA cm^{-2}. In this study, to improve the capacitance properties of the Ni−Cu-plated polyester fabric, a layer of MnO_2 was added to the surface of the flexible electrode.

In this research, a simple and rapid method was used to fabricate a flexible, high-performance, and applicable textile electrode. To achieve a highly structured supercapacitor, a flexible substrate of Ni−Cu-plated polyester fabric was employed. MnO_2 nanorods were grown directly on the fabric through a straightforward immersion process in a solution of potassium permanganate ($KMnO_4$), known for its potent oxidizing properties. The specific capacitance of the prepared electrode was examined in both symmetrical and asymmetrical cell configurations.

2. EXPERIMENTAL SECTION

2.1. Materials. In this study, 100% polyester-woven fabric with a specific weight of 80 g m^{-2} and a warp/weft density of 31/21 yarns cm^{-1} was used. Copper acetate, nickel acetate, and hydrazine were procured from Fluka Company, Switzerland, while potassium hydroxide (KOH) was obtained from Merck in Darmstadt, Germany. All other reagents were of industrial-grade purity.

2.2. Preparation of Ni−Cu/MnO_2-Plated Polyester Electrodes. In this work, nickel and copper were deposited on polyester fabric using a simplified electroless plating technique according to the method described in our previous research work.[16] It should be mentioned that the best conditions for obtaining high electrical conductivity were created on the polyester fabric. For this purpose, a solution comprising 0.1% (w/v) copper acetate and 1% (w/v) nickel acetate, along with 2.5% hydrazine as the reducing agent, was prepared. This solution was used for treating precleaned polyester fabric. Subsequently, the prepared conductive polyester was submerged in an aqueous solution of $KMnO_4$ (0.1 M) for durations of 5, 10, and 30 min at 70 °C. The Ni−Cu/MnO_2-plated polyester electrodes prepared at various deposition times of 5, 10, and 30 min were named as MnO_2/NCP-5, MnO_2/NCP-10, and MnO_2/NCP-30, respectively.

2.3. Physicochemical Characterization. The electrical resistance of the fabricated electrodes was assessed using a two-point probe method. The measurement was conducted at 10 distinct points across each electrode surface, and the average electrical resistivity was recorded. The morphology of the electrodes was examined using scanning electron microscopy (SEM) with a Czech Republic-made TESCAN VEGA3 equipped with an energy-dispersive X-ray spectroscopy (EDX) analyzer.

2.4. Manufacturing Symmetrical and Asymmetrical Supercapacitor Cells. The asymmetric supercapacitor cell (ASC) was assembled using the ideal Ni−Cu/MnO_2-plated polyester electrode (MnO_2/NCP-10) as the cathode electrode, an activated carbon-coated activated carbon cloth (ACC/AC) as the anode electrode, paired with two stainless steel meshes serving as current collectors, and a precut cellulose filter paper acting as the separator. The fabricated electrodes and separator were soaked in 6.0 M KOH aqueous solution for about 6 h before assembly. All of the cell components were sandwiched between two 1.5 × 1.5 cm^2 glasses and then tightly wrapped with a paraffin film to produce a Ni−Cu/MnO_2-plated polyester//ACC/AC cell. Then, a few drops of a 6.0 M KOH aqueous solution were injected into the fabricated cell as an electrolyte. The symmetrical supercapacitor cell (SSC) was assembled as described above, except that the Ni−Cu/MnO_2-plated polyester fabric was used as both anode and cathode. The electrochemical properties of the composite ASC and SSC were investigated.

2.5. Electrochemical Characterization. The electrochemical characteristics of the manufactured Ni−Cu/MnO_2-plated polyester fabrics were analyzed using a three-electrode cell setup at ambient temperature. To measure the specific capacitance of the prepared electrodes, cyclic voltammetry (CV) and galvanostatic charge/discharge (GCD) measurements (WonATech Zive SP1) were used. The Ni−Cu/MnO_2-plated polyester fabric acted as the working electrode, directly

https://doi.org/10.1021/acsomega.4c10183
ACS Omega 2025, 10, 7091−7101

immersed in a 1 M KOH solution. An Ag/AgCl electrode served as the reference electrode, and a platinum rod acted as the counter electrode. A constant voltage range of 0.0−0.8 V was applied to evaluate the electrochemical properties. In addition, electrochemical impedance spectroscopy (EIS) analyses were performed for all electrodes and the assembled SSC and ASC. Impedance measurements were conducted by varying the voltage around +0.3 V (near the OCV) across a frequency range of 0.01 Hz−100 kHz. The acquired EIS data were then analyzed using ZSimpWin software. Areal specific capacitances (C_a) of the electrodes were calculated based on GCD results using eq 1:

$$C_a = (i \times \Delta t)/(\Delta V \times S) \quad (1)$$

In this equation, "i" represents the constant discharge current, "Δt" stands for the discharge duration, "ΔV" denotes the operational voltage range, and "S" corresponds to the geometrical area of the electrode.[17]

3. RESULTS AND DISCUSSION

The top-down method was used in this work. In the first step, nickel and copper were deposited on polyester fabric with weight percentages of 68.5% and 20.1%, respectively, according to previously published work.[16] In the second step, MnO_2 was deposited on the surface of the Ni−Cu-plated polyester fabric by immersing it in a $KMnO_4$ solution. The electrical resistance of the fabricated flexible electrodes was assessed using a two-point probe, and the findings are presented in Table 1. As seen,

Table 1. Electrical Resistivity of the Prepared Electrodes

Samples	Average electrical resistivity (Ω cm^{-1})
MnO_2/NCP-5	3
MnO_2/NCP-10	7
MnO_2/NCP-30	40

by increasing the time of immersion of fabrics in the $KMnO_4$ solution, the electrical resistance is increased. This means that, as expected, by increasing the thickness of MnO_2 layer having has a semiconducting nature on the surface of the fabrics, the electrical resistivity is increased, see Figure 1. According to the achieved results related to electrical resistivity, sample MnO_2/NCP-10 was chosen for the rest of the experiments.

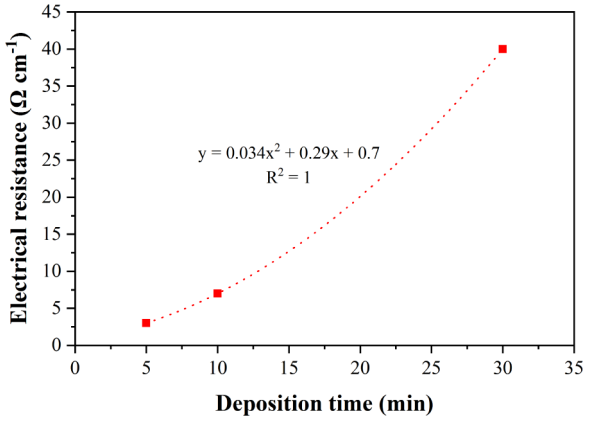

Figure 1. Electrical resistivity vs deposition time for MnO_2 deposition step.

The morphological characteristics of Ni−Cu/MnO_2-plated polyester fabric were examined and compared with untreated polyester fabric using SEM. As can be seen in Figure 2, the surface of the untreated polyester is quite smooth. At higher resolution, only a few small particles can be seen that can be associated with TiO_2, which is used in PET production.[16] After the deposition of Ni−Cu and MnO_2 on the surface of the polyester, the surface of the fibers is covered with nanostructures. According to Figure 3, during Ni−Cu plating, a layer of Ni−Cu with hedgehog-like structures, most of which are rod-shaped, was uniformly deposited around the polyester fibers. The MnO_2 nanoflowers can be clearly seen above the Ni−Cu layer. The successful deposition of MnO_2 over the Ni−Cu layer was confirmed by EDX analysis (see Figure 4). As can be seen, the weight percentages of Mn, Ni, and Cu are 4.7, 58.5, and 8.2%, respectively. The amount of Ni on the surface is higher than that of Mn and Cu, which is related to the concentration of the precursors originally used.

Initially, the electrochemical characteristics of the flexible-plated polyester samples were investigated in a three-electrode setup utilizing a 1 M KOH electrolyte. In Figure 5a, the voltammograms of MnO_2/NCP-5, MnO_2/NCP-10, and MnO_2/NCP-30 were compared. The oxidation and reduction peaks display near symmetry in each curve, indicating outstanding reversibility, enhanced conductivity, and the high capacitance of the fabricated electrode. As can be seen, the recorded current densities in MnO_2/NCP-10 are higher than those of the two other electrodes, which denotes the well electrochemical performance MnO_2/NCP-10 due to well-ordered MnO_2 nanostructures at its surface. Figure 5b−d shows the CV curves of the flexible electrodes in the range of −0.2 to +0.8 V at different sampling rates of 5, 10, 20, 40, and 80 mV s^{-1}. Basically, the same shape with a pair of clear redox peaks can be seen for all curves. The peak currents also slowly increase as the sampling rate increases. This indicates that the electron transfer kinetics on the electrodes prepared is extremely fast. As shown in Figure 5, the peak currents of the Faradaic redox reaction rise in direct correlation with the scan rate, while the CV curves retain their initial form. Conversely, at elevated scan rates, the oxidation peaks move toward more positive potentials, while the reduction peaks shift toward the negative spectrum. This means greater diffusion resistance at higher scan rates. Furthermore, at a high scan rate, even up to 80 mV s^{-1}, there is no obvious distortion in the CV diagram, indicating good speed performance and sufficient conductivity of the as-prepared electrodes. As confirmed by EDX results, the redox peaks primarily result from the reversible Faradaic reaction between Ni^{2+} and Ni^{3+}, wherein $Ni(OH)_2$ is formed during the electrochemical activation process, contributing to pseudocapacitive characteristics.[1,10,18] In the case of nickel and nickel oxide, the mechanism for charge storage primarily involves surface adsorption and redox reactions with OH^- ions, whereas for nickel hydroxide, it entails the intercalation and deintercalation of H^+ ions within the layers.[16]

The integrated area of the CV curves representing the capacitance of the electrodes is larger for MnO_2/NCP-10 than for MnO_2/NCP-5 and both are larger than that for MnO_2/NCP-30, indicating that a deposition time of 10 min suggests the optimal value for MnO_2 deposition on Ni−Cu-plated-polyester fabric. Figure 5c demonstrates significantly expanded regions of MnO_2/NCP-10 in comparison to the other two electrodes under the same scan rate of 10 mV s^{-1}. This

https://doi.org/10.1021/acsomega.4c10183
ACS Omega 2025, 10, 7091−7101

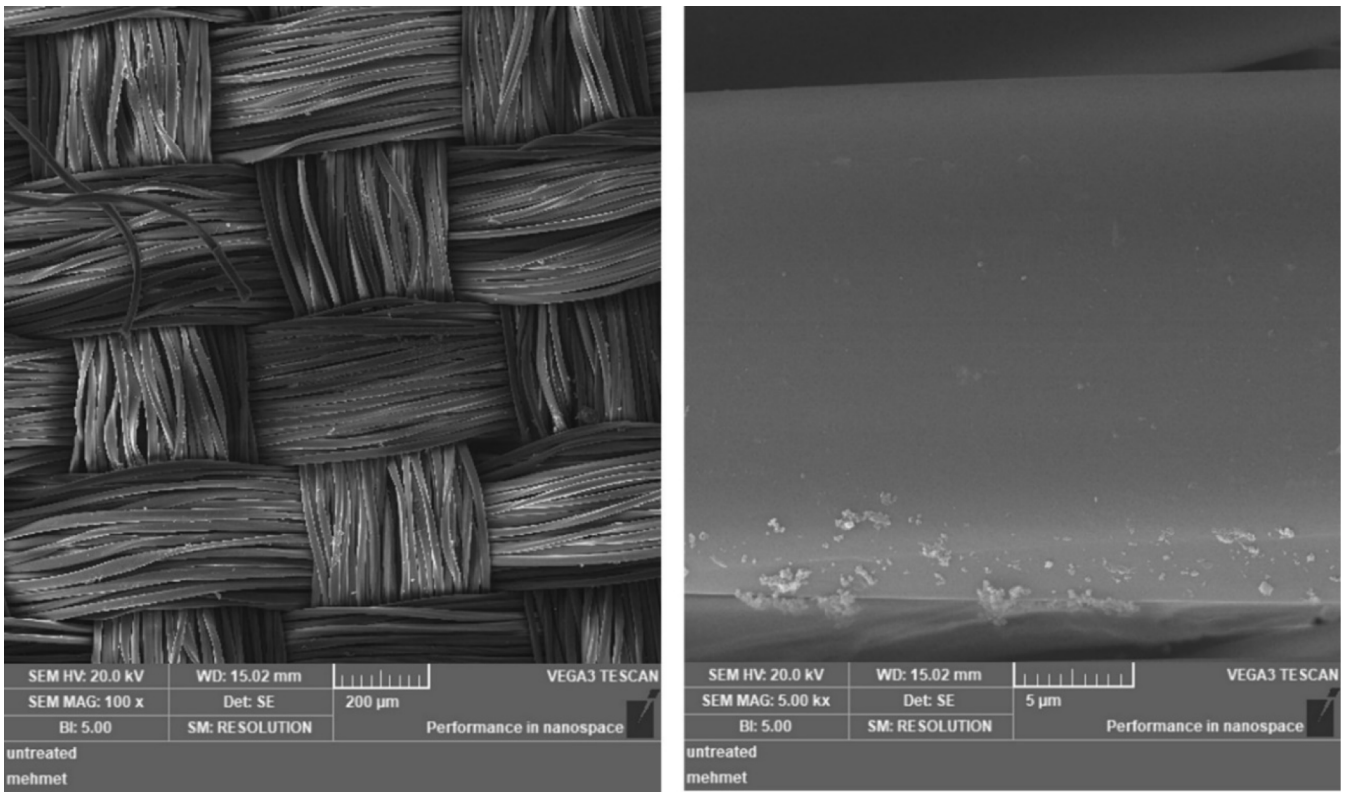

Figure 2. SEM images of untreated polyester fabric.

suggests that the capacity will be increased significantly. It is shown that MnO_2/NCP-10 has faster ionic and electron conductivity.[13] The integrated area for MnO_2/NCP-30 is not satisfactory. The electrical conductivity of MnO_2/NCP-30 is also lower than that of the other electrodes (see Table 1). In the CV curves of MnO_2/NCP-30, it is observed that complete oxidation and reduction peaks are not evident within the applied voltage window at higher scan rates, and the integrated area within these peaks is comparatively smaller than that of MnO_2/NCP-5 and MnO_2/NCP-10. Xian Li et al. concluded that a high MnO_2 loading leads to the aggregation of MnO_2 nanosheets and impairs their function. Additionally, excessive MnO_2 loading could elevate resistance and impede charge transport, as indicated by a Nyquist plot of the electrodes.[6]

The capacitance of the electrodes was determined based on the results obtained from the GCD measurements. To assess the rate capability of the treated polyester fabrics, GCD experiments were conducted under various current densities, and the corresponding graphs are depicted in Figure 6. The GCD profiles of the Ni−Cu/MnO_2-plated polyester electrodes were captured by applying current densities of 4, 8, 16, 32, and 64 mA cm^{-2} for all three electrodes. As expected, the as-prepared electrodes exhibited significantly extended charging and discharging durations under a current density of 4 mA cm^{-2}. As the current density increases to higher levels, the charge and discharge durations become shorter. Furthermore, the GCD profiles exhibit characteristics reminiscent of battery performance with two distinct potential plateaus indicating the occurrence of Faradaic redox reactions during charge and discharge processes. This observation aligns well with the findings from the CV analysis. Each discharge curve prominently displays a potential plateau corresponding to the reduction peak observed in the CV ($Ni^{3+} \rightarrow Ni^{2+}$). The excellent performance can be attributed to the tight encapsulation of small activated Ni and Mn nanoparticles within the polyester fabric, which enables rapid electron transport and easy access to the electrolyte, specifically OH^-. The wide band following the peak in the lower potential range can be attributed to the reduction of Ni^{3+} to Ni^{2+}. As a result, the fabricated electrodes can reliably operate within a wide potential range, which may be attributed to the interaction between MnO_2 and polyester, leveraging numerous functional groups present on the surface.[11,13]

The GCD curve also confirms the larger capacitance characteristics of the MnO_2/NCP-5 and MnO_2/NCP-10 electrodes due to the significantly longer discharge time. As depicted in Figure 6, the GCD curves of all the fabricated electrodes display relatively triangular shapes, suggesting efficient charge propagation between the electrodes. However, MnO_2/NCP-10 demonstrates a longer discharge time of 106 s at a current density of 4 mA cm^{-2} compared to those of both MnO_2/NCP-5 and MnO_2/NCP-30. In conclusion, extending the immersion time of the fabricated electrode in the $KMnO_4$ solution results in a decrease in the electrochemical performance of the electrode (MnO_2/NCP-30). For MnO_2/NCP-5, as the current density rises from 4 to 64 mA cm^{-2}, the areal capacitance (C_a) decreases from 640 mF cm^{-2} to 1.80 mF cm^{-2} (refer to Figure 6a). Similarly, for MnO_2/NCP-10, the areal capacitance decreases from 770 mF cm^{-2} to 23.2 mF cm^{-2}. Additionally, the areal capacitance for MnO_2/NCP-30 decreases from 487 mF cm^{-2} to nearly zero.

Figure 7 illustrates the results of electrochemical impedance spectroscopy (EIS) analyses conducted on the prepared sample electrodes. Relative to MnO_2/NCP-30, MnO_2/NCP-5 and MnO_2/NCP-10 fabric electrodes show almost a vertical trend in the high-frequency region. This indicates the fabric

https://doi.org/10.1021/acsomega.4c10183
ACS Omega 2025, 10, 7091−7101

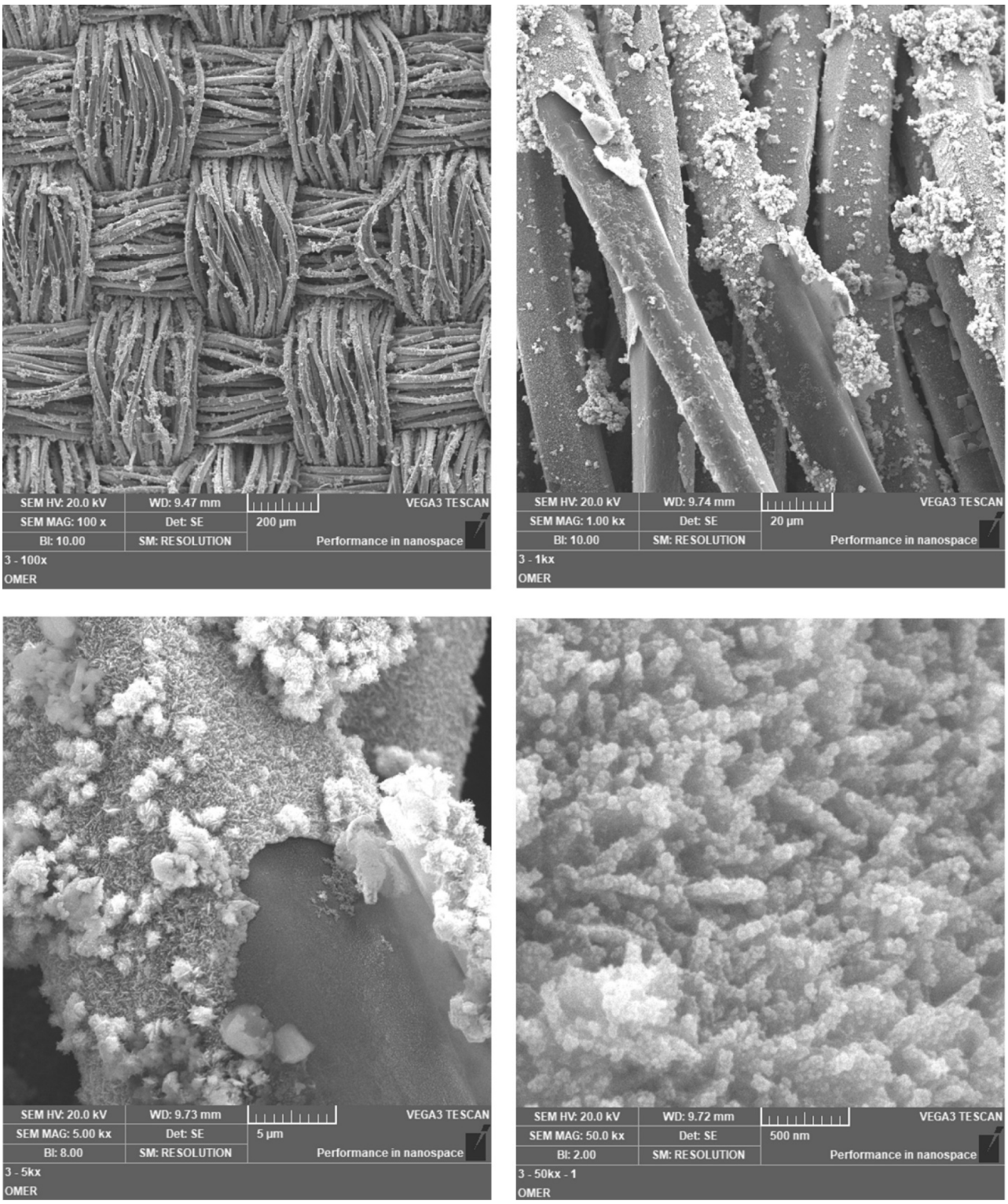

Figure 3. SEM images of MnO_2/NCP-10 at different magnifications.

electrodes' excellent electrical conductivity and minimal charge transfer resistance. Maintaining a high capacitance throughout the charge−discharge cycle is essential for enhancing the performance of the supercapacitor, which is a characteristic observed in both MnO_2/NCP-5 and MnO_2/NCP-10 electrodes. Moreover, in the EIS spectra, the inclined line observed in the low-frequency region can be attributed to Warburg impedance (Z_w), which is related to proton diffusion in the MnO_2 layer. The linear trend at low frequencies indicates the diffusion behavior of ions within the electrode structure. The porous structure of Ni−Cu/MnO_2-plated polyester electrodes enables the adsorption of water. These nanoporous areas can provide suitable diffusion channels for the electrolyte solution. Additionally, the direct contact between the internal active materials and the electrolyte reduces the diffusion distance for ions.[2] There is no distinct semicircle observed in the high-

https://doi.org/10.1021/acsomega.4c10183
ACS Omega 2025, 10, 7091−7101

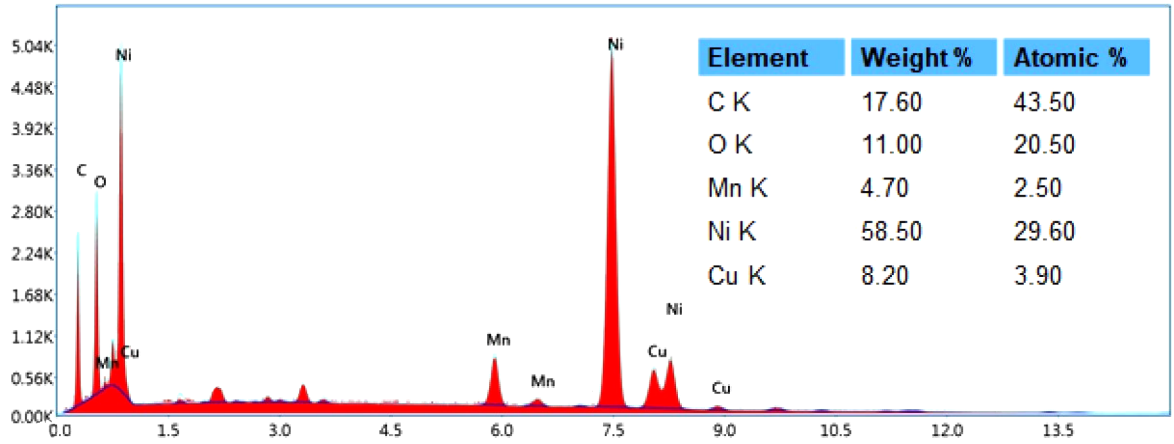

Figure 4. EDX results related to the MnO_2/NCP-10 electrode.

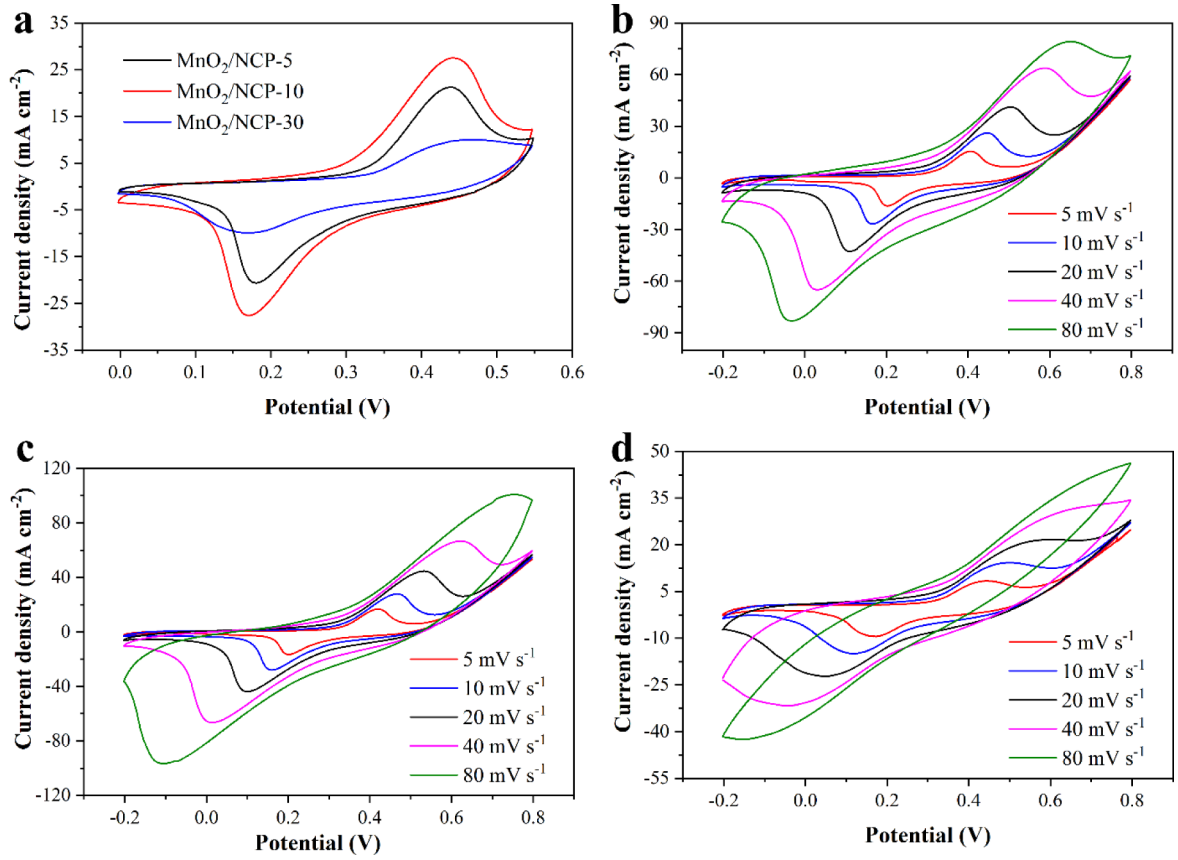

Figure 5. (a) voltammograms of the prepared electrodes at scan rate of 10 mV s^{-1} and CV curves of (b) MnO_2/NCP-5, (c) MnO_2/NCP-10, and (d) MnO_2/NCP-30 at different scan rates.

frequency region of the MnO_2/NCP-5 and MnO_2/NCP-10 electrodes. The compressed semicircle elucidates the excellent conductivity of the fabric electrodes.[11]

According to the achieved results from CV and GCD curves, it was found that the capacitance for MnO_2/NCP-10 is higher than the others. So, for the rest of the analysis and for symmetric and asymmetric cells, MnO_2/NCP-10 was chosen. Within this electrode, the integration of MnO_2 and Ni layers results in the formation of a porous structure, offering a greater active surface area for swift faradic redox reactions and facilitating the accelerated diffusion of electrolyte ions.[3] It should be mentioned again that increasing the amount of Mn on the surface of MnO_2/NCP-30 by increasing the immersion time reduces both the conductivity and the capacitance. Therefore, MnO_2/NCP-10 was selected as an optimized electrode for fabricating both symmetric and asymmetric cells.

The open spaces in the Ni−Cu/MnO_2-plated polyester fabric allow the electrolyte ions to diffuse into the inner area of the electrode. The nanorod forest, directly cultivated on polyester textile, offers a vast surface area and facilitates rapid electron transport to the current collector. The exceptional electrochemical performance of the fabricated electrodes is credited to their distinctive 3D hierarchical nanoforest-like architecture, which facilitates the swift diffusion of cations

https://doi.org/10.1021/acsomega.4c10183
ACS Omega 2025, 10, 7091−7101

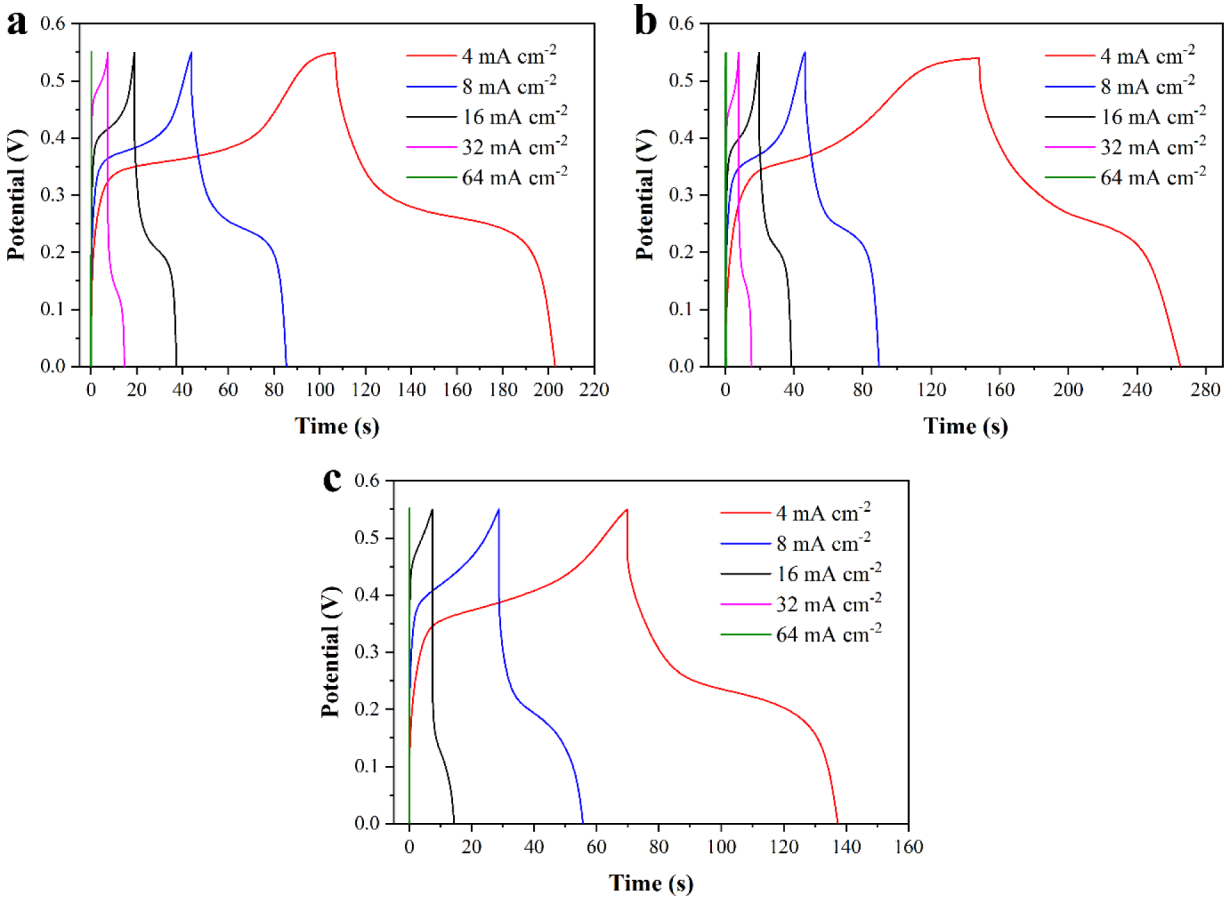

Figure 6. GCD plots of (a) MnO_2/NCP-5, (b) MnO_2/NCP-10, and (c) MnO_2/NCP-30 at various current densities.

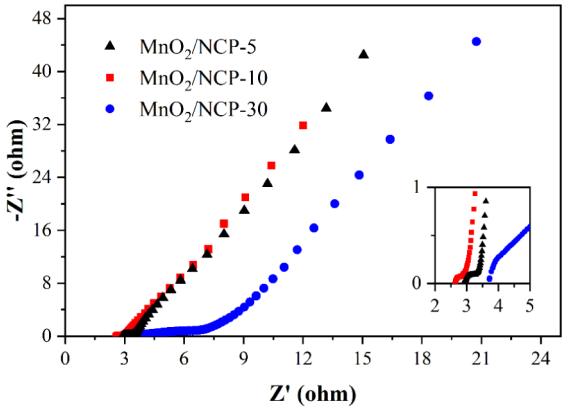

Figure 7. EIS spectra of MnO_2/NCP-5, MnO_2/NCP-10, and MnO_2/NCP-30 in 1.0 M KOH.

within the electrode during intercalation and deintercalation processes upon oxidation, thereby enhancing the rate of electrochemical reactions.[10] To explore the potential of the Ni−Cu/MnO_2-plated polyester electrode in practical applications, a symmetric cell was assembled, as depicted in Figure 8a. In the assembled symmetric cell, two MnO_2/NCP-10 pieces were employed as both anode and cathode electrodes, separated by a piece of cellulose paper to create a "sandwich" structure.

The CV response of the prepared SSC in Figure 8b showed satisfying electrochemical activity over the whole potential window. The areal capacitances (C_a) of the symmetric supercapacitor (SSC) at different current densities (0.1, 0.25, 1, and 4 mA cm^{-2}), calculated from the GCD curves displayed in Figure 8c, were 213.5, 158.7, 34.1, and 6.6 mF cm^{-2}, respectively. As previously mentioned, the notable specific capacitance of the assembled symmetric supercapacitor (SSC) at low current density can be attributed to the combined impact of the active material and the fibrous woven fabric. These factors contribute to exceptional electrical and capacitive performance, along with a high loading area.[11] In addition, the presence of nanoscale Ni−Cu/MnO_2 rods and forests (which serve as a layer on the surface of polyester fibers) helps to increase the electrochemically active surface area that electrolyte ions can access, thereby promoting ion adsorption and time migration paths of ions during the charge−discharge processes are shortened. From another perspective, the hierarchically porous Ni−Cu/MnO_2 structure served as an electrolyte reservoir, aiding in reducing the ion diffusion pathway and facilitating the efficient infiltration of electrolyte ions. In addition, the conductive Ni−Cu/MnO_2-plated polyester fabric ensured rapid electron transfer. However, as shown in Figure 8d, the SSC showed a high C_a value of 213.5 mF cm^{-2} at 0.1 mA cm^{-2}, but as the applied current density increased by 40 times, the specific surface capacitance decreased to 6.6 mF cm^{-2}. This could be attributed to the poor functionality of the Ni−Cu/MnO_2-plated polyester electrode in the anode roll, as their available capacity could not follow the rapid redox reactions of the Ni−Cu/MnO_2-plated polyester in the cathode. In addition, C_a decreases at higher current density because electrolyte ions have little time to diffuse into the inner surface of the active

https://doi.org/10.1021/acsomega.4c10183
ACS Omega 2025, 10, 7091−7101

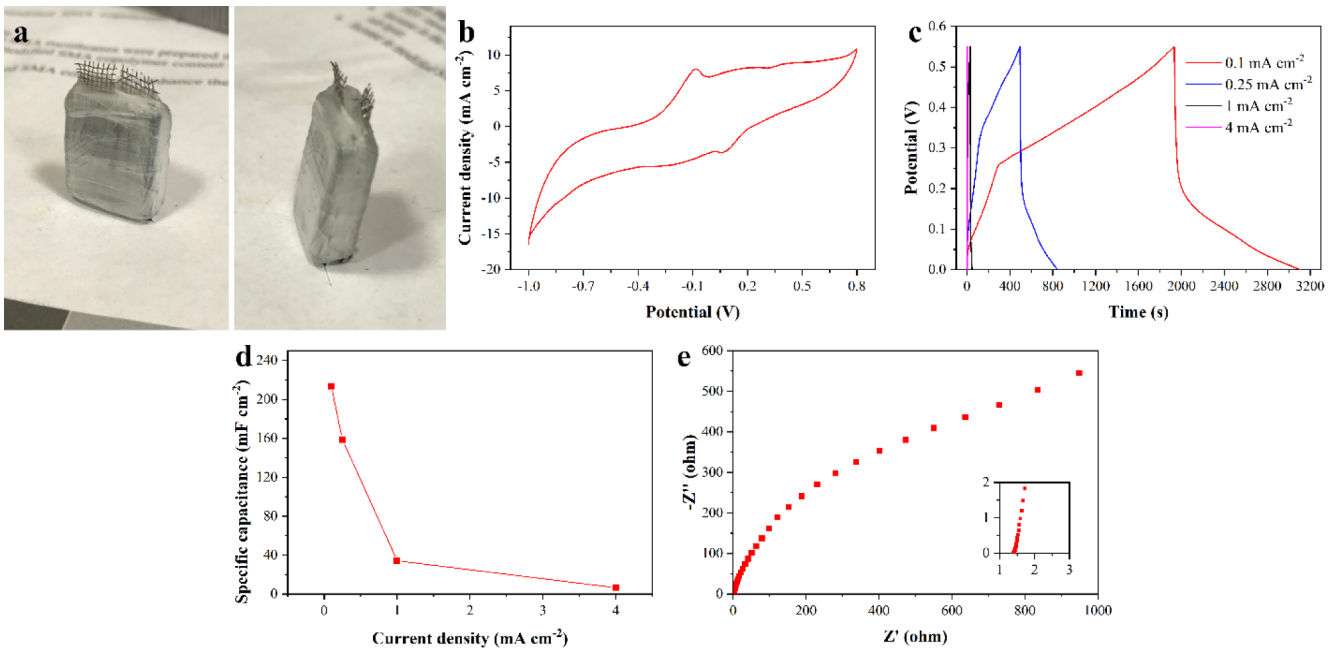

Figure 8. (a) Digital photograph, (b) CV curve at scan rate of 40 mV s^{-1}, (c) GCD curves at various current densities, (d) specific capacitances at various current densities, and (e) EIS result of the SSC.

material, whereby the limited diffusion reduces the specific capacity of the electrode material.[1,10]

However, the majority of pseudocapacitive materials cannot be employed in a symmetric supercapacitor to fully exploit their capacitance potential. Although some, such as MnO_2, can be assembled in a symmetrical configuration, the voltages of their devices are usually not high. One promising approach to enhance both the cell voltage and capacitance in aqueous electrochemical capacitors is by developing asymmetric supercapacitors (ASCs), wherein one electrode side is pseudocapacitive while the other relies on electric double-layer capacitance (EDLC). Until now, significant research endeavors have been directed toward asymmetric supercapacitors (ASCs). Transition metal oxides and hydroxides like CoO, RuO_2, MnO_2, NiO, and $Ni(OH)_2$, among others, have been extensively explored as positive electrode materials for ASCs due to their high redox electrochemical activity and ability to achieve exceptionally high capacitance.

Asymmetric supercapacitors (ASCs) provide one of the smart ways to increase energy density while maintaining power density and lifetime, based on the energy and power density formula.[18] In the present study, the ASC was fabricated by combining an ACC/AC electrode as the anode and MnO_2/NCP-10 as the cathode with KOH-impregnated cellulose paper in a single cell.

Figure 9 shows the electrochemical performance of the fabricated ASC. Separate cyclic voltammograms of the cathode and anode electrodes were examined at a scan rate of 20 mV s^{-1} in 1.0 M KOH (Figure 9a). As can be seen, the anode and cathode electrodes exhibit good capacitive behavior in their applied potential windows, suggesting that they have the potential to be assembled into an ASC. The CV curves of the as-fabricated ASC at different voltage windows are shown in Figure 9b. It is evident that the voltage window can be expanded from 0.8 to 1.4 V without exhibiting any indications of electrolysis of the electrolyte.

Figure 9c depicts the charge and discharge curves of the ASC at different current densities, including 2, 4, 8, and 16 mA cm^{-2}. The computed areal specific capacitances of the ASC were 558.6, 481.9, 435.5, and 330 mF cm^{-2} at current densities of 2, 4, 8, and 16 mA cm^{-2}, respectively. The elevated specific capacitance of the assembled ASC may be attributed to the combined impact of both the anode and cathode, contributing to outstanding electrical and capacitive performance, and the substantial loading area, as noted in reference.[11]

As shown in Figure 9d, the decrease of C_a by increasing the applied current density was much better in ASC compared to SSC (Figure 9d). The capacity retention after increasing the current density 8 times was only 60% of its value at 2 mA cm^{-2}, indicating good current capability of the fabricated ASC. The speed capability of the ASC was also evaluated using the CV technique, and the results are shown in Figure 9e. The following eq 2 can be used to explain the relationship between current density and scan rate.[19,20]

$$i = a \times v^b \tag{2}$$

where i and v are the current density and the sampling rate, respectively, and a and b are variable parameters that indicate the type of storage mechanism. When the value of b is computed as 1, indicating a linear relationship between i and v, it suggests that the redox reaction is governed by surface control. On the contrary, when the value of b is determined to be 0.5, as indicated by references,[19,20] it signifies that the redox reaction is governed by diffusion control. The recorded current densities of the anodic and cathodic peaks at different sampling rates are shown in Figure 9f. As evidenced by the calculated R-square, the correlation between current density and scan rate did not exhibit complete linearity. In this instance, the estimated value of b was approximately 0.59, suggesting that the redox reaction at the electrodes is predominantly governed by diffusion control. Furthermore, as shown in Figure 9g, the plots are completely linear, further confirming that the redox reaction is controlled by diffusion-controlled kinetics.[19,21]

https://doi.org/10.1021/acsomega.4c10183
ACS Omega 2025, 10, 7091−7101

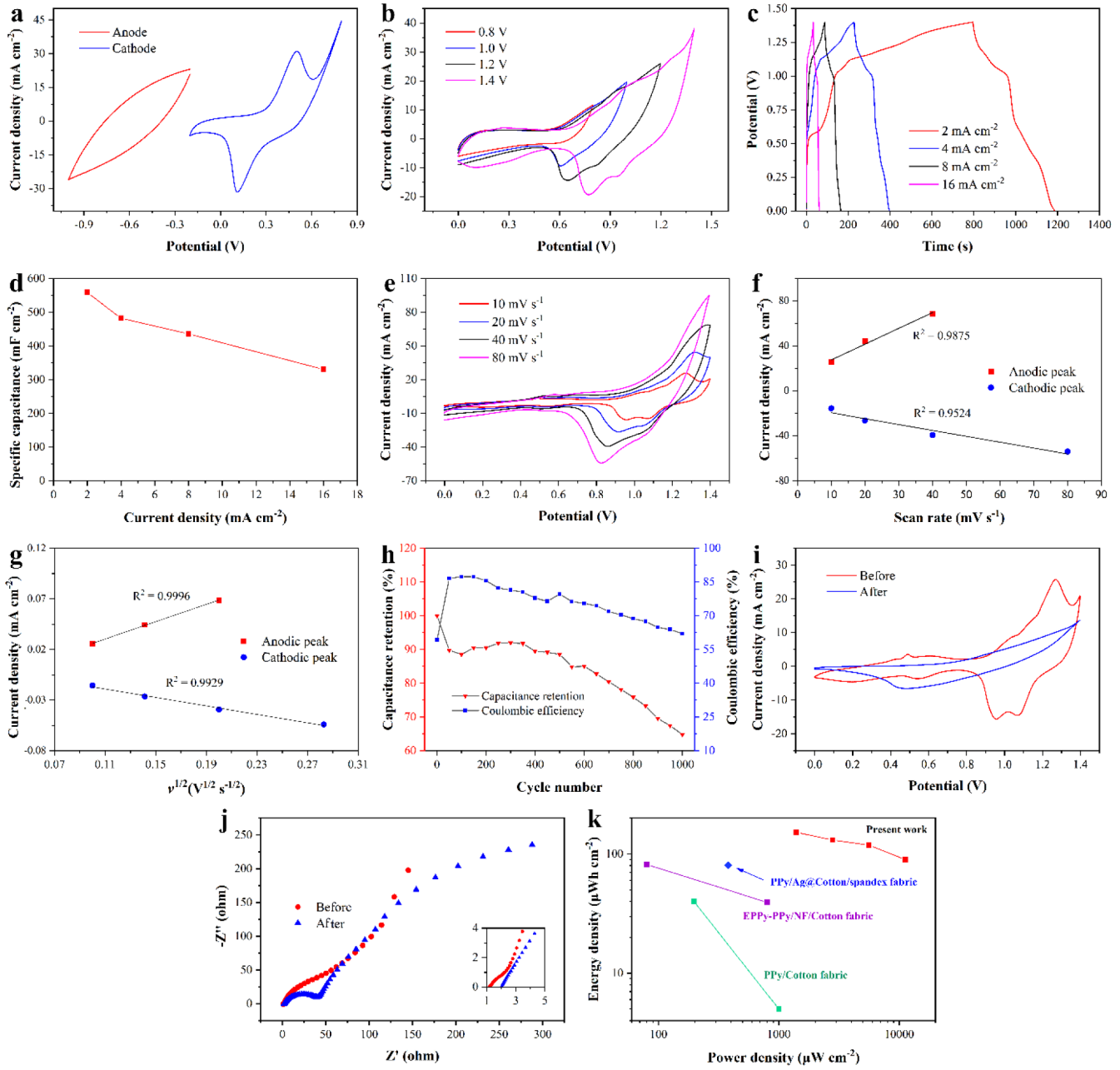

Figure 9. Electrochemical performance evaluation of the assembled ASC: CV responses of (a) cathode and anode electrodes in 1.0 M KOH and (b) the fabricated ASC at different potential windows, (c) GCD curves at various current densities, (d) specific capacitance vs current density, (e) CV curves at different scan rates, (f) current density of redox peaks vs scan rate, (g) current densities of redox peaks vs root square of scan rate, (h) cyclic stability test at 8 mA/cm^{-2}, (i) CV curves and (j) EIS spectra of the ASC before and after 1000 charge/discharge cycles, and (k) the Ragone plot of ASC.

The major mechanism responsible for the demonstrated electrochemical performance of the electrode is the contribution of metallic Ni as follows:[19]

$$Ni + 2OH^- \leftrightarrow Ni(OH)_2 + 2e^-$$

$$Ni(OH)_2 + OH^- \leftrightarrow NiOOH + H_2O + e^-$$

Besides, the MnO_2 can contribute to the electrochemical reactions occurred at the surface of the electrode according to the following equation:[25]

$$(MnO_2)\ \text{surface} + K^+ + e^- \leftrightarrow (MnO^{2-}K^+)\ \text{surface}$$

$$MnO_2 + H_2O + e^- \leftrightarrow MnOOH + OH^-$$

The changes in capacitance retention and Coulombic efficiency of the ASC during the stability test are presented in Figure 9h. As can be seen, the capacitance felt rapidly before reaching the 50th cycle, and after that, the capacitance increased a little for a few more cycles and then began to decline again. After 1000 cycles, the ASC retained 64% of its initial capacitance value. The rapid initial decline, which appeared in the first cycles, is probably due to detaching excess active materials from the electrodes. The subsequent slight increase can be attributed to exposing inner active sites of the electrode layers to electrolyte ions and hence contributed to

https://doi.org/10.1021/acsomega.4c10183
ACS Omega 2025, 10, 7091−7101

capacitance. In contrast, the Coulombic efficiency rose at the beginning of the test, which can confirm the detaching of active materials in the first few cycles. Figure 9i,j shows CV responses and EIS spectra of the ASC before and after 1000 charge and discharge cycles at a high current density of 8 mA cm^{-2}. The nearly vertical line (Figure 9j) is obtained for an asymmetric cell before 1000 charge/discharge cycles. The diameter of the semicircle in the high-frequency range (reflecting the charge transfer resistance) increased after 1000 charge and discharge cycles. As depicted in Figure 9i, the redox peaks primarily linked to the cathode surface reactions vanish after 1000 cycles, contributing to the decline in the specific capacitance of the ASC. The overall electrochemical performance of the ASC was also evaluated as the Ragone plot shown in Figure 9k. As can be seen, the fabricated ASC shows promising energy and power densities with respect to some of the reported fabric-based supercapacitors.[22−24] The fabricated ASC shows the highest energy density of 152.1 μWh cm^{-2} at a power density of 1400 μW cm^{-2} and can still provide an energy density of 89.8 μWh cm^{-2} at a high power density of 11200 μW cm^{-2}. Based on the results, the Ni−Cu/MnO_2 electrode shows promise as a cathode for the fabrication of asymmetric supercapacitors and has the potential to perform well in flexible ASCs, provided that its mechanical stability is further improved.

4. CONCLUSION

The electron transfer between the MnO_2 nanoflowers and Ni−Cu-plated polyester was facilitated by the interface connection, which was enhanced by the two-step synthesis of Ni−Cu-plated polyester and MnO_2 nanostructures, ensuring efficient electron transfer. This self-supported structure eliminated the need for a polymer binder or conductive additive in electrode preparation, thereby preventing the introduction of additional contact resistance, as noted in ref. 1 The results show that immersing Ni−Cu-plated polyester in $KMnO_4$ solution for 10 min significantly improves the capacitance properties. The existence of nanosized Ni−Cu/MnO_2 rods and forest (acting as a layer on the surface of polyester fibers) is advantageous for augmenting the electrochemically active surface area. The SSC exhibited a high capacitance area (C_a) of 213.5 mF cm^{-2} at a current density of 0.1 mA cm^{-2}. However, with a 40-fold increase in the applied current density, the areal specific capacitance decreased to 6.6 mF cm^{-2}. This could be attributed to the poor functionality of the Ni−Cu/MnO_2-plated polyester electrodes in the anode role, as their available capacity could not follow the rapid redox reactions of the Ni−Cu/MnO_2-plated polyester in the cathode.

The asymmetric supercapacitor cell (ASC), consisting of a Ni−Cu/MnO_2-plated polyester fabric, i.e., MnO_2/NCP-10, as the cathode electrode and an activated carbon-coated activated carbon fabric (ACC/AC) as the anode electrode, has a high area specificity with capacities of 558.6 mF cm^{-2} at current densities of 2 mA cm^{-2}. The elevated specific capacitance of the assembled ASC may stem from the combined impact of both the anode and cathode, along with the fibrous structure of the polyester fabric.

AUTHOR INFORMATION

Corresponding Author

Rattanaphol Mongkholrattanasit − *Department of Textile Chemistry Technology, Faculty of Industrial Textiles and Fashion Design, Rajamangala University of Technology Phra Nakhon, Bangkok 10300, Thailand;* orcid.org/0000-0003-3288-910X; Email: rattanaphol.m@rmutp.ac.th

Authors

Sheila Shahidi − *Department of Textile, Faculty of Engineering and Agriculture, Islamic Azad University, Arak Branch, Arak 38361-1-9131, Iran*

Fatma Kalaoglu − *Department of Textile Engineering, Faculty of Textile Technologies and Design, Istanbul Technical University, Istanbul 34437, Turkey*

Leila Naji − *Department of Chemistry, Amirkabir University of Technology (Tehran Polytechnic), Tehran 15916-3-4311, Iran;* orcid.org/0000-0003-1593-2751

Alireza Rahmanian − *Department of Chemistry, Amirkabir University of Technology (Tehran Polytechnic), Tehran 15916-3-4311, Iran*

Complete contact information is available at: https://pubs.acs.org/10.1021/acsomega.4c10183

Author Contributions

This research has seen significant contributions from all authors, each playing a distinct role; S.S.: Conceptualization, writing—original draft preparation, writing—review and editing; S.S. and F.K.: Investigation, Formal analysis; S.S. and L.N.: Methodology, Data curation; L.N.: Methodology, Formal analysis; L.N. and A.R.: Data curation, Discussion, Review; A.R.: Discussion, Review; R.M.: Conceptualization, writing—review and editing, supervision. All authors have read and approved the final manuscript.

Notes

The authors declare no competing financial interest.

ACKNOWLEDGMENTS

The authors express their gratitude to Rajamangala University of Technology Phra Nakhon (RMUTP), Thailand; Islamic Azad University, Arak, Iran; Istanbul Technical University, Istanbul, Turkey, and Amirkabir University of Technology (Tehran Polytechnic), Tehran, Iran, for their support in this research. This research did not receive any specific grant from funding agencies in the public, commercial, or not-for-profit sectors.

REFERENCES

(1) Wan, C.; Jiao, Y.; Liang, D.; Wu, Y.; Li, J. A high-performance, all-textile and spirally wound asymmetric supercapacitors based on core−sheath structured MnO_2 nanoribbons and cotton-derived carbon cloth. *Electrochim. Acta* **2018**, *285*, 262−271.

(2) Ullah, S.; Yu, J.; Liu, H.; Iqbal, W.; Yang, B.; Li, C.; Zhu, C.; Xu, J. Fabrication of MnO_2-carbonized cotton yarn derived hierarchical porous active carbon flexible supercapacitor electrodes for potential applications in cable-type devices. *Appl. Surf. Sci.* **2019**, *487*, 180−188.

(3) Guo, M. X.; Bian, S. W.; Shao, F.; Liu, S.; Peng, Y. H. Hydrothermal synthesis and electrochemical performance of MnO_2/graphene/polyester composite electrode materials for flexible supercapacitors. *Electrochim. Acta* **2016**, *209*, 486−497.

(4) Wang, Z.; Wang, H.; Ji, S.; Wang, H.; Brett, D. J. L.; Wang, R. Design and synthesis of tremella-like Ni−Co−S flakes on co-coated cotton textile as high-performance electrode for flexible supercapacitor. *J. Alloys Compd.* **2020**, *814*, 151789.

(5) Wen, J.; Xu, B.; Zhou, J.; Chen, Y. Novel high-performance asymmetric supercapacitors based on nickel-cobalt composite and PPy for flexible and wearable energy storage. *J. Power Sources* **2018**, *402*, 91−98.

(6) Li, G. X.; Hou, P. X.; Luan, J.; Li, J. C.; Li, X.; Wang, H.; Shi, C.; Liu, C.; Cheng, H. M. A MnO_2 nanosheet/single-wall carbon nanotube hybrid fiber for wearable solid-state supercapacitors. *Carbon* **2018**, *140*, 634−643.
(7) Lu, J.; Wan, H.; Ju, T.; Ying, Z.; Zhang, W.; Li, B.; Zhang, Y. Super flexible electrospun carbon/nickel nanofibrous film electrode for supercapacitors. *J. Alloys Compd.* **2019**, *774*, 593−600.
(8) Wei, H.; Hu, H.; Feng, J.; Zhang, M.; Hua, T. Yarn-form electrodes with high capacitance and cycling stability based on hierarchical nanostructured nickel-cobalt mixed oxides for weavable fiber-shaped supercapacitors. *J. Power Sources* **2018**, *400*, 157−166.
(9) Jiang, Y.; Zhou, C.; Liu, J. A non-polarity flexible asymmetric supercapacitor with nickel nanoparticle@ carbon nanotube three-dimensional network electrodes. *Energy Storage Mater.* **2018**, *11*, 75−82.
(10) Shah, H. U.; Wang, F.; Javed, M. S.; Ahmad, M. A.; Saleem, M.; Zhan, J.; Khan, Z. U. H.; Li, Y. In-situ growth of MnO_2 nanorods forest on carbon textile as efficient electrode material for supercapacitors. *J. Energy Storage* **2018**, *17*, 318−326.
(11) Li, Z.; Tian, M.; Sun, X.; Zhao, H.; Zhu, S.; Zhang, X. Flexible all-solid planar fibrous cellulose nonwoven fabric-based supercapacitor via capillarity-assisted graphene/MnO_2 assembly. *J. Alloys Compd.* **2019**, *782*, 986−994.
(12) Zhang, J.; Sun, J.; Shifa, T. A.; Wang, D.; Wu, X.; Cui, Y. Hierarchical MnO_2/activated carbon cloth electrode prepared by synchronized electrochemical activation and oxidation for flexible asymmetric supercapacitors. *Chem. Eng. J.* **2019**, *372*, 1047−1055.
(13) Wang, Y.; Li, X.; Wang, Y.; Liu, Y.; Bai, Y.; Liu, R.; Yuan, G. High-performance flexible MnO_2@ carbonized cotton textile electrodes for enlarged operating potential window symmetrical supercapacitors. *Electrochim. Acta* **2019**, *299*, 12−18.
(14) Zhou, R.; Fu, Y.; Chao, K. A.; Cheng, C. H. Green synthesis of nanoarchitectured nickel fabrics as high performance electrodes for supercapacitors. *Renewable Energy* **2019**, *135*, 1445−1451.
(15) Paleo, A. J.; Staiti, P.; Brigandì, A.; Ferreira, F. N.; Rocha, A. M.; Lufrano, F. Supercapacitors based on AC/MnO_2 deposited onto dip-coated carbon nanofiber cotton fabric electrodes. *Energy Storage Mater.* **2018**, *12*, 204−215.
(16) Shahidi, S.; Kalaoglu, F. In situ deposition of nickel nano particles on polyester fabric and its application as a flexible electrode in supercapacitor. *J. Ind. Text.* **2022**, *51*, 4913S.
(17) Rahmanian, A.; Naji, L. Systematic study of influencing parameters on the in-situ electrochemical growth of three-dimensional graphene on carbon cloth for supercapacitor applications. *J. Energy Storage* **2022**, *49*, 104146.
(18) Jeon, H.; Jeong, J.-M.; Hong, S. B.; Yang, M.; Park, J.; Kim, D. H.; Hwang, S. Y.; Choi, B. G. Facile and fast microwave-assisted fabrication of activated and porous carbon cloth composites with graphene and MnO_2 for flexible asymmetric supercapacitors. *Electrochim. Acta* **2018**, *280*, 9−16.
(19) Rahmanian, A.; Naji, L. Graphene oxide-assisted electrochemical growth of Ni $(OH)_2$ nanoflowers on nickel foam as electrode material for high-performance supercapacitors. *Colloids Surf., A* **2022**, *640*, 128450.
(20) Tian, Z.; Wang, X.; Li, B.; Li, H.; Wu, Y. High rate capability electrode constructed by anchoring $CuCo_2S_4$ on graphene aerogel skeleton toward quasi-solid-state supercapacitor. *Electrochim. Acta* **2019**, *298*, 321−329.
(21) Shahrokhian, S.; Mohammadi, R.; Asadian, E. One-step fabrication of electrochemically reduced graphene oxide/nickel oxide composite for binder-free supercapacitors. *Int. J. Hydrogen Energy* **2016**, *41*, 17496−17505.
(22) Lv, J.; Liu, Z.; Zhang, L.; Li, K.; Zhang, S.; Xu, H.; Mao, Z.; Zhang, H.; Chen, J.; Pan, G. Multifunctional polypyrrole and rose-like silver flower-decorated E-textile with outstanding pressure/strain sensing and energy storage performance. *Chem. Eng. J.* **2022**, *427*, 130823.
(23) Sun, D.; Liu, Q.; Yi, C.; Chen, J.; Wang, D.; Wang, Y.; Liu, X.; Li, M.; Liu, K.; Zhou, P.; Sun, G. The construction of sea urchin spines-like polypyrrole arrays on cotton-based fabric electrode via a facile electropolymerization for high performance flexible solid-state supercapacitors. *Electrochim. Acta* **2020**, *354*, 136746.
(24) Wang, B.; Song, W.; Gu, P.; Fan, L.; Yin, Y.; Wang, C. A stretchable and hydrophobic polypyrrole/knitted cotton fabric electrode for all-solid-state supercapacitor with excellent strain capacitance. *Electrochim. Acta* **2019**, *297*, 794−804.
(25) Wang, H. Q.; Yang, G. F.; Li, Q. Y.; Zhong, X. X.; Wang, F. P.; Li, Z.-S.; Li, Z. H. Porous nano-MnO_2: large scale synthesis via a facile quick-redox procedure and application in a supercapacitor. *New J. Chem.* **2011**, *35*, 469−475.

https://doi.org/10.1021/acsomega.4c10183
ACS Omega 2025, 10, 7091−7101